An analytical model to determine equilibrium quantities of azimuthally symmetric and mismatched charged particle beams under linear focusing

R. P. Nunes, R. Pakter, and F. B. Rizzato

Citation: Journal of Applied Physics **104**, 013302 (2008); doi: 10.1063/1.2949270
View online: http://dx.doi.org/10.1063/1.2949270
View Table of Contents: http://scitation.aip.org/content/aip/journal/jap/104/1?ver=pdfcov
Published by the AIP Publishing

An analytical model to determine equilibrium quantities of azimuthally symmetric and mismatched charged particle beams under linear focusing

R. P. Nunes,[a] R. Pakter, and F. B. Rizzato
Instituto de Física, Universidade Federal do Rio Grande do Sul, Av. Bento Gonçalves 9500, Caixa Postal 15051, CEP 91501-970, Porto Alegre, Rio Grande do Sul, Brazil

(Received 3 December 2007; accepted 25 April 2008; published online 3 July 2008)

The model developed here analytically allows to obtain equilibrium quantities of interest from high-intensity charged particle beams such as the emittance, beam envelope, and the number of beam halo particles. The results obtained in this work have been particularized to the case of initially homogeneous beams, with azimuthal symmetry, and focused by a constant magnetic field while confined in a linear channel. For validation, full self-consistent *N*-particle beam simulations have been carried out and its results compared with the predictions supplied by the developed hybrid numerical-analytical model. The agreement has been reasonable. Also, the model revealed to be useful to understand the basic physical aspects of the problem. © *2008 American Institute of Physics*. [DOI: 10.1063/1.2949270]

I. INTRODUCTION

Beams with any given initial distribution of charged particles confined by a magnetic focusing system can relax from a nonstationary into a stationary state through the increasing of one of its statistical quantities known as emittance.[1] This is the case of the system of interest here: azimuthally symmetric beams with initially mismatched envelopes, flowing along the symmetry axis of the focusing channel permeated by an axial magnetic field. To better understand the emittance growth above, Jameson[2] proposed a model in which the interaction of individual particles with the beam is analyzed. Gluckstern analytically solved[3] this particle-core model and has shown that the physical mechanism possibly related to this emittance growth is large resonant islands[4] beyond the beam border.

The formation of these resonant islands is induced by the initial mismatch of the beam, which can drive particles residing in the beam vicinity to excursions with high amplitude. From the point of view of energy conservation, the resonant coupling above progressively converts energy of the beam macroscopic oscillation into kinetic energy associated with the microscopic chaotic movement of the outer particles, causing the decay of the beam envelope and, as a consequence, the increasing of its emittance. This process continues until the equilibrium state of the system is reached, at which moment the emittance saturates. In this situation, looking at the beam phase-space, the particles that compose the beam can be mainly classified in two distinct populations: a dense one, formed by low velocity particles which compose the beam core, and a tenuous one, surrounding the previous population and formed by high velocity particles, which compose what is known as the beam halo. This splitting of the beam distribution in these two distinct populations naturally appears in the full self-consistent *N*-particle simulations of mismatched beams, as will be shown in the next sections of this work.

It is important here to explain that the meaning of the words stationary and equilibrium used until here, and hereafter, is related to the beam phase-space. The stationary or equilibrium state should be understood as the situation in which the topology of the beam phase-space is unchanged as time evolves. In this case, there is no more energy exchange between the particles that compose the beam halo and the particles that compose the beam core, indicating that the decay of the beam envelope has ceased due to the inexistence of free energy in the overall system. This just implies that the geometry of the beam phase-space is explicitly invariant with the time. This concept will become clearer in Sec. III B of this work, where a deeper discussion will take place.

The beam halo formation has implications over engineering aspects of accelerators since it can cause radioactivation[5] of its confinement structure, resulting in a possible damage of its electronic components and precluding the human maintenance. Also, these beam losses increase the costs with maintenance of the experimental apparatus and degrade the beam quality, which is a requisite for some applications. In this way, investigations that intend to characterize the beam halo are an important issue to build the next-generation high-power machines.

From the accelerator engineering point of view, a satisfactory characterization of the beam halo is achieved with the determination of its maximum spatial dimension and the time scale of its formation, as the beam mismatch varies. With the first information, to say the spatial dimension of the beam halo, it is possible to better design the conducting pipes employed in the magnetic confinement system while with the second information, the time scale of the beam halo formation, it is possible to design a more efficient collimation system for the accelerator. However, considering the physics point of view, other information such as the density of particles that composes the beam halo and the beam emittance is also of interest. These last quantities help to better under-

[a]Electronic mail: rogerpn@if.ufrgs.br.

stand the mechanisms behind the halo formation, its influence over the beam core, and as a consequence, its influence over the overall dynamics of the beam.

The purpose of the current article is to better detail and to extend previous results firstly introduced in Ref. 6 and afterward in Ref. 7, which has been mainly dedicated to develop a semianalytical model for estimation of the time scales of the beam halo formation as function of the initial beam mismatch. In this article, it will be described in detail a method to analytically determine beam equilibrium quantities such as emittance, envelope, and number of halo particles of an azimuthally symmetric beam with respect to its initial mismatch. For simplification of the calculations as well as for a clearer explanation, the beam has been considered initially homogeneous. Through the model, it has been found that only with a few assumptions about the geometry of the initial and the final beam phase-space aided by general equations for the conserved quantities of the entire system, composed by the particles and fields, the above commented quantities can be naturally evaluated as function of the initial beam mismatch. For validation, the developed model will be compared with full self-consistent *N*-particle beam simulations, considering several values of initial beam mismatches.

This article is organized in the following form: in Sec. II, the general equations employed in the analytical model developed are briefly reviewed. It is interesting here to emphasize that these equations describe macroscopic quantities of beams with arbitrary phase-space distributions. In Sec. III, the analytical model developed is formally described and presented. For simplicity of the calculation, a beam initially without emittance (a cold beam) and initially with a homogeneous density (step-function profile) has been considered. In Sec. IV, the results provided by our model, namely, the beam emittance, the beam envelope, and the number of beam halo particles at the beam equilibrium state, are compared with full self-consistent *N*-particle simulations, based on the Gauss' law. To assure the model validity, the previous commented comparison has been done for several values of initial beam mismatch, such as 20%, 40%, 60%, 80%, and 100%. Finally, in Sec. V, the conclusions of this article and the perspectives for futures works will be discussed.

II. GENERAL EQUATIONS

Notwithstanding the complexity of the beam dynamics, some equations for conserved quantities of the beam distribution can still be obtained. This is the case of charged particle beams with arbitrary particle distributions flowing in a linear acceleration channel. The channel is encapsulated by a conducting pipe with circular cross section, which is permeated by a solenoidal magnetic field aligned to the pipe symmetry axis. The presence here of a conducting pipe has key importance in assuring that the overall beam canonical angular momentum is conserved, independent of the azimuthal characteristics of the beam distribution. For the rms beam radius

$$R_b(s) \equiv \langle x^2 + y^2 \rangle^{1/2}, \tag{1}$$

in which the angular brackets denote phase-space averaging, one of these above commented equations can be established[8]

$$\frac{d^2R_b(s)}{ds^2} + \kappa_z(s)R_b(s) - \frac{K(1+\Delta_b)}{2R_b(s)} - \frac{\varepsilon^2(s)}{4R_b^3(s)} = 0, \tag{2}$$

in which $k_z(s)=[qB_z(s)/2\gamma m\beta c^2]^2$ is the focusing factor and $B_z(s)$ denotes the axial and s-dependent focusing magnetic field. $K=2Nq^2/\gamma^3 m\beta^2 c^2$ is the constant beam perveance, and $\Delta_b = 1/2\pi K^2 \int_0^{2\pi} (r(\partial/\partial r)\delta\psi)^2|_{r=r_w} d\theta$ computes the azimuthal distortions in the beam distribution represented by angular fluctuations of the dimensionless scalar electromagnetic potential $\delta\psi$. $\varepsilon(s)$ is the beam emittance, which can depend on the axial distance s. N is the number of beam particles per unit axial length (which is constant), q denotes the beam particles charge, m is the corresponding particle mass, $\gamma = (1-\beta^2)^{-1/2}$ is the relativistic factor, $\beta = v_z/c$, in which v_z is the constant axial beam velocity, and c denotes the speed of light. s is the axial coordinate and is directly related to the time t through $s=s_0+\beta ct$. All spatial variables are in the Larmor frame. For this reason, time and axial distance here has the same meaning from the point of view of the equations.

The beam emittance is defined in the form

$$\varepsilon^2(s) = 4\left(\langle x^2 + y^2 \rangle \langle x'^2 + y'^2 \rangle - \frac{\langle x^2 + y^2 \rangle'^2}{4} \right), \tag{3}$$

in which the primes indicate derivatives with respect to the axial distance s. Equation (3) only defines a statistical quantity of the beam distribution. The global balance of the beam's energy can be expressed by[8]

$$\frac{d}{ds}\left(\frac{1}{2}\langle x'^2 + y'^2 \rangle + \frac{\kappa_z(s)}{2}\langle x^2 + y^2 \rangle + \mathcal{E}(s) \right) = \frac{1}{2}\langle x^2 + y^2 \rangle \frac{dx_z(s)}{ds}. \tag{4}$$

This one will prove useful later to connect the initial nonstationary beam state with its final stationary state, in the light of the analytical model developed and subsequently described in Sec. III. In Eq. (4), $\mathcal{E}(s)$ is the dimensionless self-field beam energy given by

$$\mathcal{E}(s) = \frac{1}{4\pi K}\int |\nabla\psi|^2 d^2r, \tag{5}$$

in which ψ is the already above commented dimensionless scalar electromagnetic potential governed by the Poisson equation

$$\nabla_\perp^2 \psi = -\frac{2\pi K}{N} n(\mathbf{r},s), \tag{6}$$

in which $n(\mathbf{r},s)$ represents the beam's particle density, the symbol $\perp$ indicates that the operation is carried out over the transverse spatial coordinates, and the dimensionless scalar electromagnetic potential ψ is scaled with units of $\gamma^3 m\beta^2 c^2/q$.

It is interesting to emphasize here that the above equations, namely, Eqs. (1)–(6), are valid for any value of s, during all the beam dynamics, irrespective of the kind of the beam distribution. This is assured by imposing that the beam evolves inside a circular conducting pipe.

Thus, it can be observed that if one now supplements Eqs. (1)–(6) with the initial condition at beam entrance, which consists of establishing the initial beam distribution, and with additional information about the same beam distribution in its equilibrium, it becomes possible to estimate the beam quantities desired here such as emittance, envelope, and the number of halo particles on the stationary state as a function of the beam's initial mismatch. This will be the subject of Sec. III.

III. THE DEVELOPED MODEL

In order to simplify the calculations done right after in the next subsections, some definitions about the initial beam shape and the employed magnetic focusing field will be made. In this work, it will be considered the case of azimuthally symmetric beams, focalized by a constant solenoidal magnetic field, which, respectively, implies that

$$\Delta_b = 0, \quad \text{and } \kappa_z(s) = \kappa. \tag{7}$$

Also considering a beam with an initial step-function profile, it is possible to introduce

$$r_b(s) = \sqrt{2} R_b(s), \tag{8}$$

in which $r_b(s)$ designates the beam envelope.

Inserting the conditions presented in Eqs. (7) and (8) into Eq. (2), the following equation for the beam envelope arises,

$$\frac{d^2 r_b(s)}{ds^2} + \kappa r_b(s) - \frac{K}{r_b(s)} - \frac{\varepsilon^2(s)}{r_b^3(s)} = 0. \tag{9}$$

In the same way, inserting these Eqs. (7) and (8) into Eq. (4) readily gives the energy conservation equation below

$$\frac{1}{2}\langle x'^2 + y'^2 \rangle + \frac{\kappa}{2}\langle x^2 + y^2 \rangle + \mathcal{E}(s) = \text{const}. \tag{10}$$

To leave the system depending on just one free parameter, namely, the beam initial mismatch, it is interesting to use a scaling scheme in all previous described equations of this article. A way to do so is to rescale all transverse coordinates in units of the beam equilibrium radius, defined as $r_{\text{eq}} = \sqrt{K/\kappa}$, and rescale the longitudinal coordinate in units of $1/\sqrt{\kappa}$. As a consequence of using this rescaling technique, the emittance is now given by units of $K/\kappa^{1/2}$. All of this is exactly equivalent to set $K \to 1$ and $\kappa \to 1$ in all equations in which these parameters appear, and that has been enunciated until here in this article.

As will be possible to infer in the subsections below, the simplification above will not restrict the application of the developed model to other beam shapes and magnetic focusing systems. This model is somewhat more general because it involves conserved quantities of the beam, whose equations are valid for the overall dynamics inside the focusing channel. The initial beam distribution is just an initial condition, and the type of magnetic focusing field is just a parameter, which has to be inserted as an input in the developed model. However, the assumptions in this section are very useful to clarify how the model works. Especially is the consideration about the magnetic focusing field, which yields directly the simple energy conservation equation (10).

With the support of the previous equations, the task resides in just to connect the beam's initial nonstationary state with the beam's final stationary state. This link between the final and initial beam's state is crucial to evaluate the stationary beam quantities of interest here as functions of the unique initial free parameter in the model, the beam initial mismatch.

A. The beam nonstationary state

The system considered here is composed by a beam of charged particles of radius $r_c(s)$, with an initial circular cross section, and moving along the symmetry axis of an inner channel of a circular conducting pipe of radius r_w. The beam is initially cold, which means that its initial emittance can be neglected. In this case, the beam is space charge dominated, and since space-charge beams are fairly homogeneous,[1] it is possible to suppose that the initial beam's distribution satisfies a step-function profile

$$n(\mathbf{r}, s=0) \equiv n_0 = \begin{cases} N/\pi r_0^2 & \text{for } r \leqslant r_0 \\ 0 & \text{for } r_0 < r \leqslant r_w, \end{cases} \tag{11}$$

in which r is the radial coordinate measured from the symmetry axis of the pipe and $r_0 = r_c(s=0)$ denotes the initial value for the beam envelope, which under the action of the rescaling procedure adopted above is nothing more than the beam initial mismatch.

Defining the initial beam density, which is described by Eq. (11), it is possible to evaluate its initial scalar electromagnetic potential ψ or its derivatives related to the transversal coordinate r. Inserting Eq. (11) into Eq. (6) and solving the resulting ordinary differential equation for the self-consistent electric field $\mathbf{E}$, which depends only on r due to the problem's symmetry, one has

$$E_r(\mathbf{r}, s=0) \equiv E_{r0} = \begin{cases} r/r_0^2 & \text{for } r \leqslant r_0 \\ 1/r & \text{for } r_0 < r \leqslant r_w, \end{cases} \tag{12}$$

in which E_r is the radial component of the self-consistent electric field $\mathbf{E}$.

Knowing the expression for the electric field self-generated by the beam density of charged particles, its energy contribution can be computed. Inserting Eq. (12) into Eq. (5) yields

$$\mathcal{E}(s=0) \equiv \mathcal{E}_0 = -\tfrac{1}{2}\ln(r_0) + \tfrac{1}{2}\ln(r_w) + \tfrac{1}{8}. \tag{13}$$

Since the emittance of the initial beam distribution has been set to zero, by a reason that has been previously elucidated, information about the initial kinetic energy of the beam's particles can be determined. Imposing $\varepsilon(s=0)=0$ in Eq. (3), using Eqs. (1) and (8), and considering that $r_b(s=0)=r_0$ reads, respectively, that

$$\langle x'^2 + y'^2\rangle(s=0) = 0, \quad \text{and} \quad \langle x^2 + y^2\rangle(s=0) = r_0^2/2. \tag{14}$$

By the possession of Eqs. (13) and (14), one is able to evaluate the final expression for the energy conservation equation (10), which reads

$$\frac{r_0^2}{4} - \frac{1}{2}\ln(r_0) + \frac{1}{2}\ln(r_w) + \frac{1}{8} = \text{const} = E(s=0) \equiv E_0. \tag{15}$$

This is the initial beam energy E_0, which has to be conserved as time evolves, independent of the evolution of the beam profile and everything else. Note also that this quantity depends only on the just one free parameter of the developed model: the initial beam mismatch. The term dependent on r_w is not a problem. In fact, this one should be canceled out with its analogous part originated from the calculation of the final stationary state. The next task resides in analyzing the beam equilibrium.

B. The beam stationary state

As the beam envelope evolves inside the focusing channel, particles begin to observe the action of nonlinear forces that start to transfer energy from the beam envelope oscillation to the motion of individual particles, which are expelled from the beam core and initiate to populate an extended hot halo of radius $r_h(s)$, larger than the beam core $r_c(s)$. These high-energetic particles surround the cold beam core, having their motion coupled with this through Gluckstern's resonances. At this point, expression (11) is clearly no longer valid, since not only particles are not restricted to live within the beam envelope $r_c(s)$ but also because the profile of the beam density changes in such a way that this one becomes considerably inhomogeneous. This additional complexity can be included in the beam dynamics as a splitting of the beam density $n(\mathbf{r},s)$ in two distinct densities, one for the particles of the beam halo $n_h(\mathbf{r},s)$ and other one for the particles of the beam core $n_c(\mathbf{r},s)$.

After this kind of instability is originated, the beam envelope suffers an abrupt decay, moving itself toward a new state, in which it will remain. As a matter of fact, this does not occur as s goes to the infinity, but in a finite time scale τ,[7] which ideally depends on the initial beam mismatch r_0. This new state is an equilibrium one, in such terms as described in Sec. I, the introduction of this article. In this stationary state, the geometry of the beam phase-space is explicitly invariant with the time s and Eq. (11) can be updated to

$$n(\mathbf{r}, s \geqslant \tau) \equiv n_\tau = \begin{cases} n_c(\mathbf{r}) + n_h(\mathbf{r}) & \text{for } r \leqslant r_c \\ n_h(\mathbf{r}) & \text{for } r_c < r \leqslant r_h \\ 0 & \text{for } r_h < r \leqslant r_w, \end{cases} \tag{16}$$

in which the time dependence does not have to be explicited anymore, and $n_c(\mathbf{r})$ continues to obey a step-function profile like in Eq. (11).

Such as can be observed in Eq. (16), the problem resides on just to calculate the halo density $n_h(\mathbf{r})$. To determine this one, it is necessary to include some external information about the beam profile at equilibrium. With the help of full self-consistent N-particle beam simulations, it has been remarked that, for $s \geqslant \tau$, the particles that compose the beam halo live in a specific region of the beam phase-space. Moreover, this phase-space region has a regular geometry, which can be readily converted to analytical expression. Additionally, this is expected to be unchanged for every time $s \geqslant \tau$, as has been written in this article.

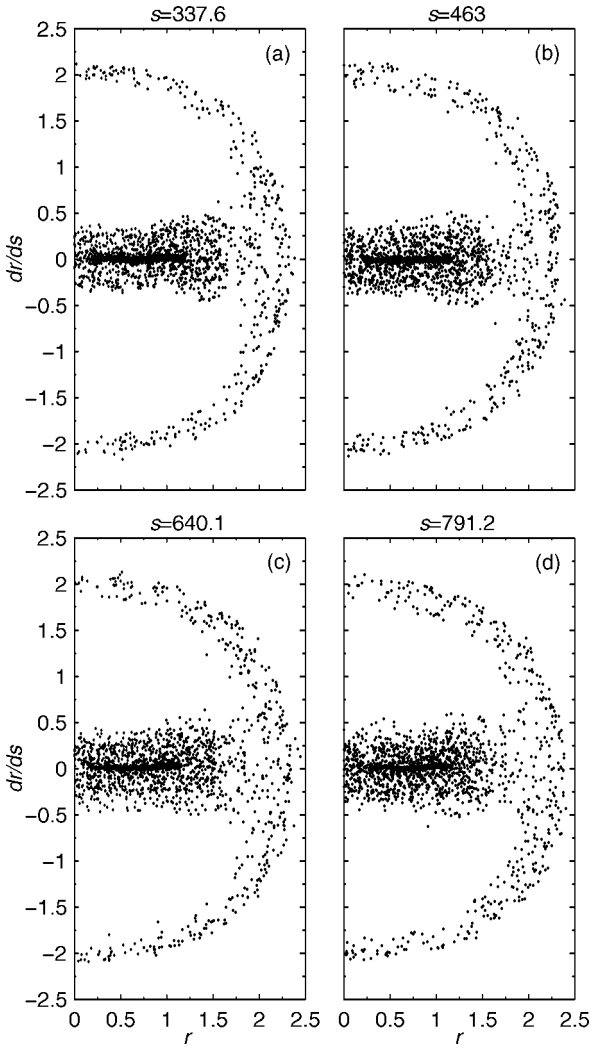

FIG. 1. Several snapshots of the transverse beam phase-space during its dynamics for an initial beam mismatch of $r_0=1.6$. Snapshots at (a) $s=337.6$, (b) $s=463$, (c) $s=640.1$, and (d) $s=791.2$.

In Fig. 1, four snapshots of the beam phase-space at different times of the beam dynamics after $s \geqslant \tau$ are shown. These ones are a result of full self-consistent N-particle beam simulations carried out until $s=800$ for $N=10\,000$ particles and an initial beam mismatch of $r_0=1.6$. The first one of these snapshots has been captured at $s=337.6$, and is shown in Fig. 1(a), right after the beam envelope decay. The other ones are presented in Fig. 1(b) at $s=463.0$, in Fig. 1(c) at $s=640.1$, and in Fig. 1(d) at $s=791.2$. From these snapshots it is possible to observe that the geometry of the beam phase-space is almost invariant, which is in accordance with the previous definition of equilibrium done in Sec. I. Also, it is possible to identify beam particles which lie in two distinct regions of the beam phase-space: extremely hot particles over a semicircular branch, which will be named here as

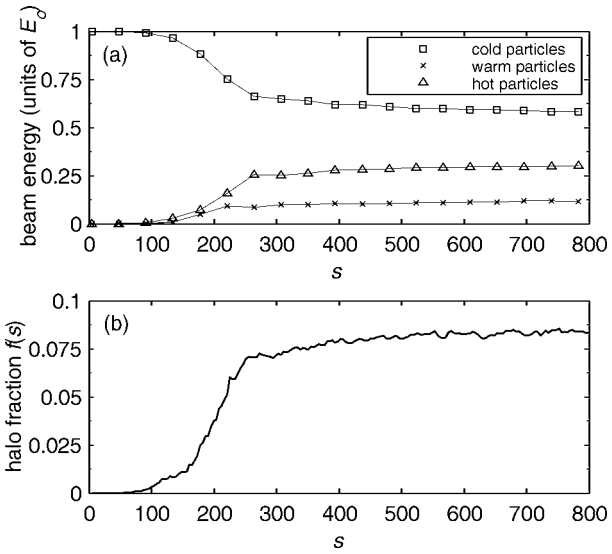

FIG. 2. The partition of the beam energy between cold, warm, and hot particles as a function of the time s is shown in panel (a). In panel (b), the time dependence of the fraction $f(s)$ of the beam halo particles is shown. All panels have been constructed for an initial beam mismatch of $r_0=1.6$. For this case, $E_0\cong 0.5294$.

beam halo particles, and cold particles over a horizontal branch, which will be named here as beam core particles.

In fact, a sharper look at the beam phase-space of Figs. 1(a)–1(d) will identify a cloud of warm particles around the cold beam core. However, these particles have been neglected in the analytical model developed in this subsection for the beam stationary state. The reason for this is that its density is too low when compared with the particle density of the beam core. Also, although its density is greater than the one of beam halo particles, it has so much less energy, a fact that can be explained since these particles do not resonantly interact with the beam core. Without this resonant coupling, the warm particles are not able to extract energy from the beam envelope oscillation and convert it to kinetic energy of its individual motion. This is in accordance with what is shown in Fig. 2(a), in which the energy carried by the cold, warm, and hot particles is shown along the time s for the same previous beam initial mismatch $r_0=1.6$. The energy for each type of particle has been normalized by the initial beam energy, which, for the present mismatch, has the value $E_0=0.5294$. It can be seen that initially all the beam energy is stored in its cold particles. However, after a time, some particles become warm, being soon some of these ones immediately captured and excited by the nonlinear resonances. There is thus a coupling between the movements of the cold particles with the hot ones. This process is fast and rapidly drains a large amount of energy from the cold particles, directing the system to its stationary state. In this state, there is not anymore energy flux between core and halo particles. At the equilibrium, the cold particles contribute with approximately 58%, the hot ones with 30%, and the warm ones with 12% of the overall beam energy. This fact justifies the option previously adopted of not taking into account the contribution of the warm particles at the equilibrium in the model to be developed.

For the particles that reside on the semicircular branch, it is possible to write an analytical expression for the halo's density formally given by

$$\lambda_h(r)=\int_{r_i'}^{r_f'}\sigma(r,r')dr, \tag{17}$$

in which $\sigma(r,r')$ is the density of particles lying in the semicircular branch of the beam phase-space, and r_f'-$r_i'\equiv w$ defines the width of the semicircular branch. Again, by a visual inspection of the beam phase-space, it is possible to approximate $\sigma(r,r')\approx\sigma$ and, since w is too small front of the beam halo dimensions, Eq. (17) can be simply written as

$$\lambda_h(r)\approx\frac{2\sigma r_h w}{\sqrt{r_h^2-r^2}}, \tag{18}$$

in which r_h is the size of the beam halo obtained from the beam phase-space with $r_h=r_i'(r=0)$. It should be noted that $\lambda_h(r)$ is a linear density and must be converted to a superficial density for solving the Poisson equation (6). With this last remark in mind and noticing that the quantity $2\sigma r_h w$ can be expressed in terms of the halo fraction $f\equiv N_h/N$ through the equation $N_h=\int_0^{r_w}\lambda_h(r)dr$, the final expression for the density of beam halo particles is achieved,

$$n_h(r)=\frac{fN}{\pi^2 r\sqrt{r_h^2-r^2}}. \tag{19}$$

In this model, the fraction f represents the influences of the halo particles over the beam dynamics. More specifically, this fraction is the weight factor of the reaction of the halo particles over the core particles, which can be associated with the amount of energy transferred from the beam core to the beam halo. At the beam equilibrium, this quantity is expected to be constant. To demonstrate this, the time evolution of the halo fraction f has been plotted in Fig. 2(b). The fraction f, as expected, starts with zero at $s=0$ until $s\approx\tau=200$, moment when there is a sharp transition in its value. After this, the fraction f stabilizes again, now at the asymptotic value in which this will remain: the equilibrium value. Note the similarity between the time dependence of the fraction f shown in Fig. 2(b) with the one for the energy of hot particles shown in Fig. 2(a). The growth of both is directly related.

With the beam density thus modeled, it is possible, adopting the same procedure of Sec. III A, to evaluate the energy stored in the electromagnetic field originated from the entire beam density of charged particles at its stationary state. Considering Eq. (16) with the aid of Eq. (19) and inserting the resulting expression in the Poisson equation (6), the electric field is promptly obtained,

$$E_r(\mathbf{r}, s \geqslant \tau) \equiv E_{r\tau} = \begin{cases} E_{r\tau,0-c} = -\dfrac{(1-f)r}{r_c^2} - \dfrac{2f}{\pi r}\arctan\left(\dfrac{r}{\sqrt{r_h^2 - r^2}}\right) & \text{for } r \leqslant r_c \\ E_{r\tau,c-h} = -\dfrac{2f}{\pi r}\arctan\left(\dfrac{r}{\sqrt{r_h^2 - r^2}}\right) - \dfrac{(1-f)}{r} & \text{for } r_c < r \leqslant r_h \\ E_{r\tau,h-w} = -\dfrac{1}{r} & \text{for } r_h < r \leqslant r_w, \end{cases} \tag{20}$$

in which $E_{r\tau,0\text{-}c}$ is the electric field in the core region, $E_{r\tau,c\text{-}h}$ is the electric field in the halo region, and $E_{r\tau,h\text{-}w}$ is the electric field in the vacuum region. The energy of the above electric field is obtained inserting Eq. (20) into Eq. (5),

$$\mathcal{E}(s \geqslant \tau) \equiv \mathcal{E}_\tau = \frac{1}{2}\left(\int_0^{r_c} |E_{r\tau,0-c}|^2 r dr + \int_{r_c}^{r_h} |E_{r\tau,c-h}|^2 r dr\right) + \frac{1}{2}\ln(r_w) - \frac{1}{2}\ln(r_h), \tag{21}$$

in which the integrals above are only indicated and must be solved numerically, since no analytical solution for these expressions has been found yet.

In the stationary state, the derivatives of beam quantities in relation to the axial coordinate can be taken as zero. This fact is a consequence of the criteria adopted in this work about the geometric invariance of the beam phase-space, which has been corroborated here in this subsection by the beam phase-space snapshots shown in Figs. 1(a)–1(d). Thus, without loss of generality, in the stationary state $d/ds\langle x^2 + y^2\rangle(s \geqslant \tau) = 0$ can be taken, which determines that in this state equation (9) becomes

$$-r_b^4(s \geqslant \tau) + r_b^2(s \geqslant \tau) + \varepsilon^2(s \geqslant \tau) = 0, \tag{22}$$

and Eq. (3) becomes

$$\varepsilon^2(s \geqslant \tau) = 2r_b^2(s \geqslant \tau)\langle x'^2 + y'^2\rangle(s \geqslant \tau). \tag{23}$$

Isolating the emittance ε^2 term in Eq. (22) and inserting this in Eq. (23), the quantity $\langle x'^2 + y'^2\rangle(s \geqslant \tau)$ can be obtained in terms of r_b^2 in the form

$$\langle x'^2 + y'^2\rangle(s \geqslant \tau) = \frac{r_b^2(s \geqslant \tau) - 1}{2}. \tag{24}$$

With this last result given by Eq. (24), the energy conservation equation (10) assumes the following format at equilibrium:

$$\frac{r_b^2(s \geqslant \tau)}{2} - \frac{1}{4} + \mathcal{E}_\tau = \text{const}. \tag{25}$$

With the beam halo and the beam core densities determined, it is possible to evaluate in the equilibrium the expression for the beam envelope $r_b(s \geqslant \tau)$. From the point of view of the beam phase-space of Fig. 1, and considering Eqs. (8) and (9), the phase-space average takes the important form

$$r_b^2(s \geqslant \tau) = (1-f)2\langle x^2 + y^2\rangle_c + f2\langle x^2 + y^2\rangle_h = (1-f)r_c^2 + fr_h^2, \tag{26}$$

in which the averages have been broke up in contributions from the beam core and beam halo, and evaluated with the help of the previous determined densities. Equation (26) propitiates that the emittance ε^2 term and the average kinetic energy $1/2\langle x'^2 + y'^2\rangle$ term in the equilibrium can be determined as a function of the beam phase-space parameters here defined as r_h and r_c and through Eqs. (22) and (23). In Sec. III C, the connection between the stationary and the nonstationary beam state will be done.

C. Connection between the nonstationary and the stationary beam state

After the modeling done for the beam stationary state, which has propitiated that the energy stored in its field and in its particles had been computed, it is possible to connect this state with the initial nonstationary beam state. Crudely, from the point of view of the expressions of Secs. III A and III B, this means to relate the initial beam mismatch r_0 with the final equilibrium parameters r_c and r_h of the beam phase-space. Thus, connecting Eq. (25) to Eq. (15), with the help of Eq. (26) for the beam envelope r_b and Eq. (21) for the beam self-field energy $\varepsilon(s)$, both at the equilibrium, one has

$$\int_0^{r_c} |E_{r\tau,0-c}|^2 r dr + \int_{r_c}^{r_h} |E_{r\tau,c-h}|^2 r dr - fr_c^2 = \frac{r_0^2}{2} - r_c^2 - r_h^2 + \ln\left(\frac{r_h}{r_0}\right) + \frac{3}{4}, \tag{27}$$

in which $E_{r\tau,0\text{-}c}$ and $E_{r\tau,c\text{-}h}$ have been already previously defined in Eq. (20). Note also that the terms depending on the pipe wall coordinate r_w naturally disappear in this equation once that its contributions are equal in any connected beam states. This is valid during the entire beam dynamics.

In Eq. (27) above, the terms depending on the fraction f of beam halo particles are grouped in the left side while the terms explicitly depending on the stationary and nonstationary beam state parameters are grouped in the right side. As it has been commented in Sec. III B, the integrals in Eq. (27) have to be solved numerically, since no analytical solution has been found yet. Extracting the parameters r_0 and (r_c, r_h), respectively, from the nonstationary and stationary beam state, and making use of these as an input in Eq. (27), one is able to achieve a second-order polynomial in the fraction f,

TABLE I. Comparison between the results provided by the developed analytical model and the results obtained from full self-consistent N-particle beam simulations.

	$r_0=1$	$r_0=1.2$	$r_0=1.4$	$r_0=1.6$	$r_0=1.8$	$r_0=2.0$
r_c	=1	≅1.05	≅1.10	≅1.10	≅1.20	≅1.20
r_h	=0	≅1.5	≅1.88	≅2.00	≅2.13	≅2.25
$A(r_c,r_h)$	=0	≅−0.199 51	≅−0.375 183	≅−0.377 568	≅−0.404 318	≅−0.402 654
$B(r_c,r_h)$	=1	≅−1.465 28	≅−3.334 149	≅−3.974 192	≅−4.805 143	≅−5.505 915
$C(r_0,r_c,r_h)$	=0	≅0.012 67	≅0.156 393	≅0.324 309	≅0.640 634	≅0.985 397
f_{model}	=0	≅0.008 63	≅0.046 66	≅0.080 98	≅0.131 85	≅0.176 68
f_{simul}	=0	≅0.020 80	≅0.051 81	≅0.083 53	≅0.132 86	≅0.177 92
$\varepsilon_{\text{model}}$	=0	≅0.276 17	≅0.540 21	≅0.851 04	≅1.188 55	≅1.572 64
$\varepsilon_{\text{simul}}$	=0	≅0.235 35	≅0.453 12	≅0.764 91	≅1.120 57	≅1.504 50
$r_{b\ \text{model}}$	=1	≅1.034 99	≅1.111 79	≅1.219 44	≅1.337 70	≅1.466 36
$r_{b\ \text{simul}}$	=1	≅1.028 93	≅1.080 63	≅1.167 17	≅1.283 89	≅1.405 07

$$A(r_c,r_h)f^2 + B(r_c,r_h)f + C(r_0,r_c,r_h) = 0, \tag{28}$$

in which the dependence of the polynomial's coefficients has been left explicitly as a function of the beam phase-space parameters r_0, r_c, and r_h. Just one solution has physical meaning, since the fraction of beam halo particles should satisfy $0 \leqslant f \leqslant 1$. Note again that the coefficients A, B, and C in the above equation must be solved numerically, since the integrands of Eq. (27) are so complicated. Further efforts have to be dispensed to solve these integrals analytically. However, its functional dependence is explicit, once the expressions for the electric field in the inner region of the focusing channel are known and described by Eq. (20) at equilibrium. Further information in this issue will be available in Ref. 9.

As will be seen in Sec. IV, the geometry of the beam phase-space remains almost unchanged with respect to the initial beam mismatch. This suggests that the beam halo distribution described by Eq. (19), and as a consequence all calculations done in Secs. III C and III B, can be extended, with reasonable accuracy, to the determination of the beam quantities of interest here for all the mismatch values considered in the next section of this work.

Thus, considering that the initial beam mismatch r_0 and the final beam phase-space parameters (r_c,r_h) are known values to obtain the desired equilibrium quantities such as the fraction of halo particles f, the beam envelope $r_b(s \geqslant \tau)$, and the beam emittance $\varepsilon(s \geqslant \tau)$, one has to follow, as a resume of all that has been done in this subsection, the algorithm below:

(1) Solve Eq. (27) for the beam halo fraction f and look for the positive root of the polynomial of Eq. (28).
(2) Insert the fraction f determined in Step (1) into Eq. (26) to determine the beam envelope $r_b(s \geqslant \tau)$.
(3) Insert the beam envelope $r_b(s \geqslant \tau)$ determined in Step (2) into Eq. (24) to evaluate the quantity $\langle x'^2+y'^2\rangle(s \geqslant \tau)$.
(4) Finally, to obtain the beam emittance $\varepsilon(s \geqslant \tau)$ at equilibrium, insert the quantities $\langle x'^2+y'^2\rangle(s \geqslant \tau)$ and $r_b(s \geqslant \tau)$ determined, respectively, in Steps (3) and (2) into Eq. (23).

Observe that the (r_c,r_h) parameters can be acquired directly from the beam phase-space or simply by visual inspection of its equivalent particle-core model obtained from a cumulative Poincaré section.[6] Further useful information will be found in Ref. 10.

IV. RESULTS AND COMPARISON WITH SIMULATIONS

To assure the validity of the developed model, formally presented in the previous section, self-consistent N-particle beam simulations have been carried out for several values of the initial beam mismatch r_0. Due to the azimuthal symmetry of the beam, the method of simulation employed here has been through the Gauss' law: the force observed by a particle at a radial coordinate r depends just on the number of particles with radial coordinates smaller than r.[7] This method is also suitable here because it includes only collective effects, since particles interact with each other through just its generated electromagnetic fields. A total number of $N=10\,000$ particles has been employed in the numerical simulations, the number of particle this that has been shown to assure convergence in the results. The total beam energy has been monitored during all the executed self-consistent N-particle beam simulations.

All results of the analytical model developed are summarized and compared with the full self-consistent simulations in Table I. In its first two rows, the values of the beam phase-space parameters (r_c,r_h) at equilibrium as function of the initial beam mismatch r_0 which appears in this same table as columns, are presented. These values have been obtained from several snapshots of the beam phase-space generated by the full self-consistent N-particle beam simulations described above. They are shown in panel (b) of Fig. 3 for $r_0=1.2$, in panels (a) and (c) of Fig. 4 for $r_0=1.4$ and $r_0=1.6$, respectively, and also in panels (a) and (c) of Fig. 5, for, respectively, $r_0=1.8$ and $r_0=2.0$. With these (r_c,r_h) values, it has been possible to determine the polynomial coefficients of Eq. (28) for each one of the initial beam mismatch r_0, using the algorithm previously commented at the end of Sec. III C.

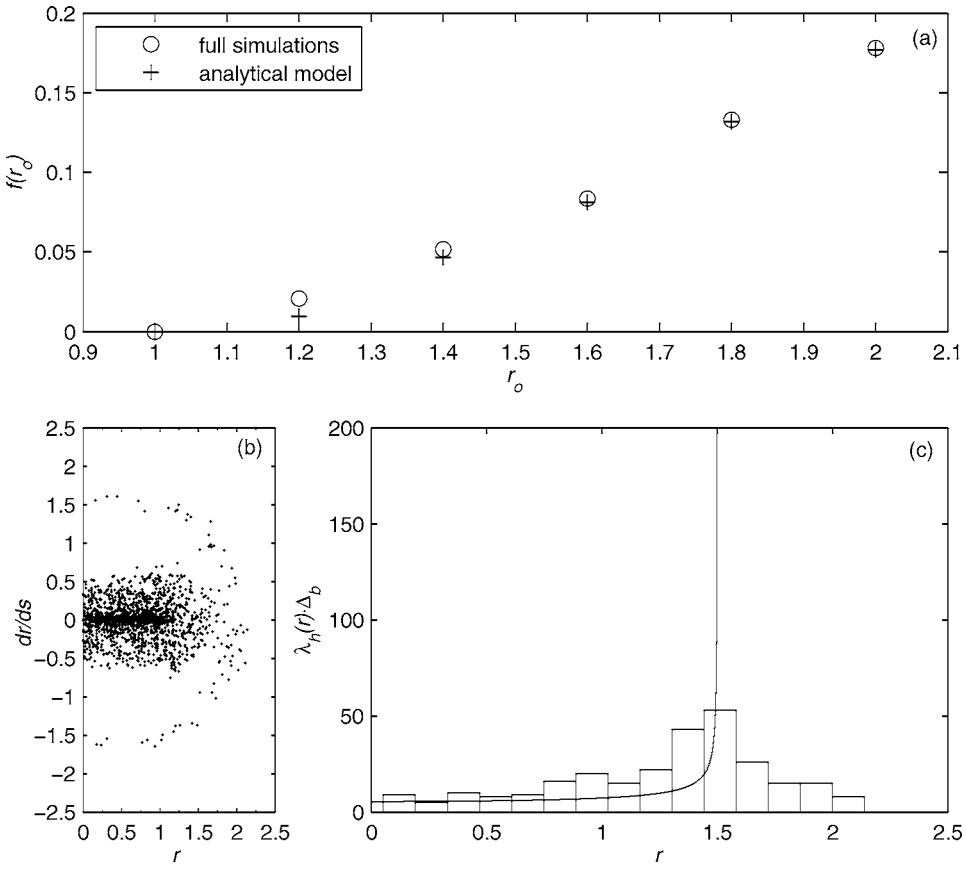

FIG. 3. (a) Comparison between the fraction of halo particles f computed through the full self-consistent N-particle simulation and the developed analytical model. In panel (b), the beam phase-space at $s \cong 1600$ for $r_0 = 1.2$ is shown. The histogram of beam halo particles for this mismatch is shown in panel (c), in which the analytical model is also plotted for comparison. $\Delta_b = 0.1390$ is the size of the bins employed in the histogram.

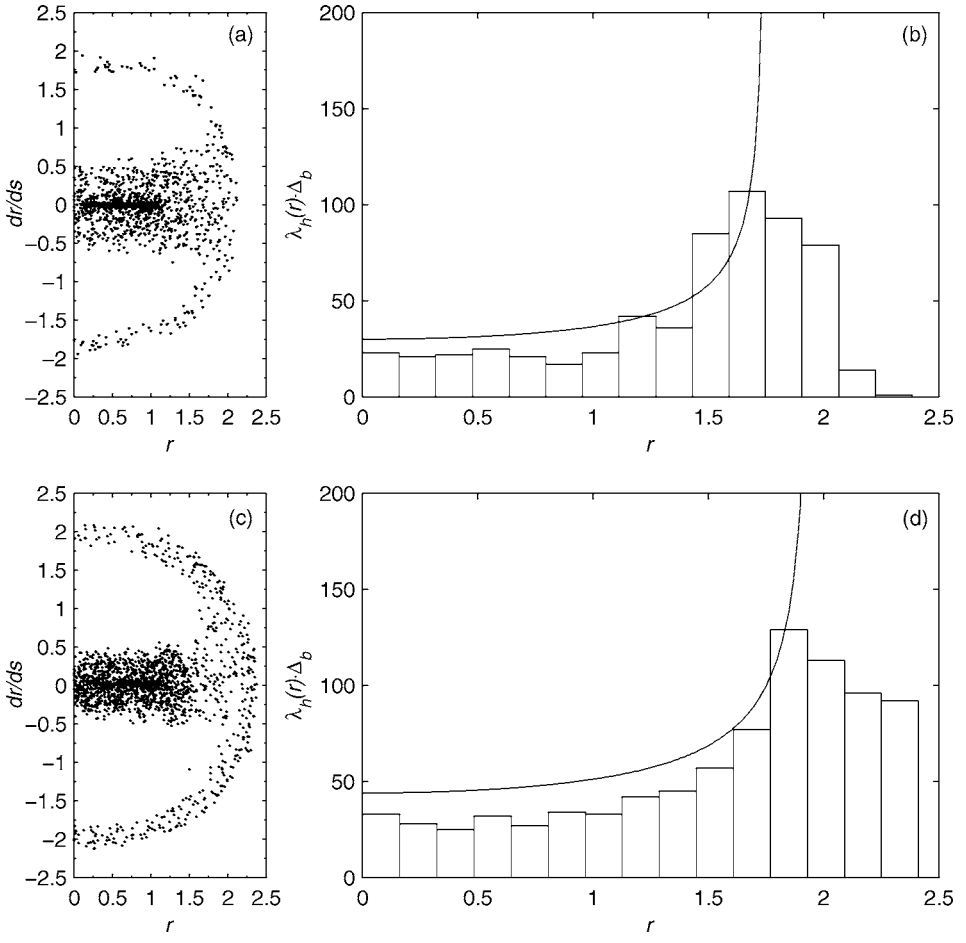

FIG. 4. phase-spaces corresponding to the full self-consistent N-particle simulations at $s \cong 800$ for (a) $r_0 = 1.4$ and (c) $r_0 = 1.6$. The histograms of beam halo particles for each one of these mismatches are, respectively, shown in panels (b) and (d), in which the analytical model is also plotted for comparison. $\Delta_b = 0.1589$ is the size of the bins employed in the histograms.

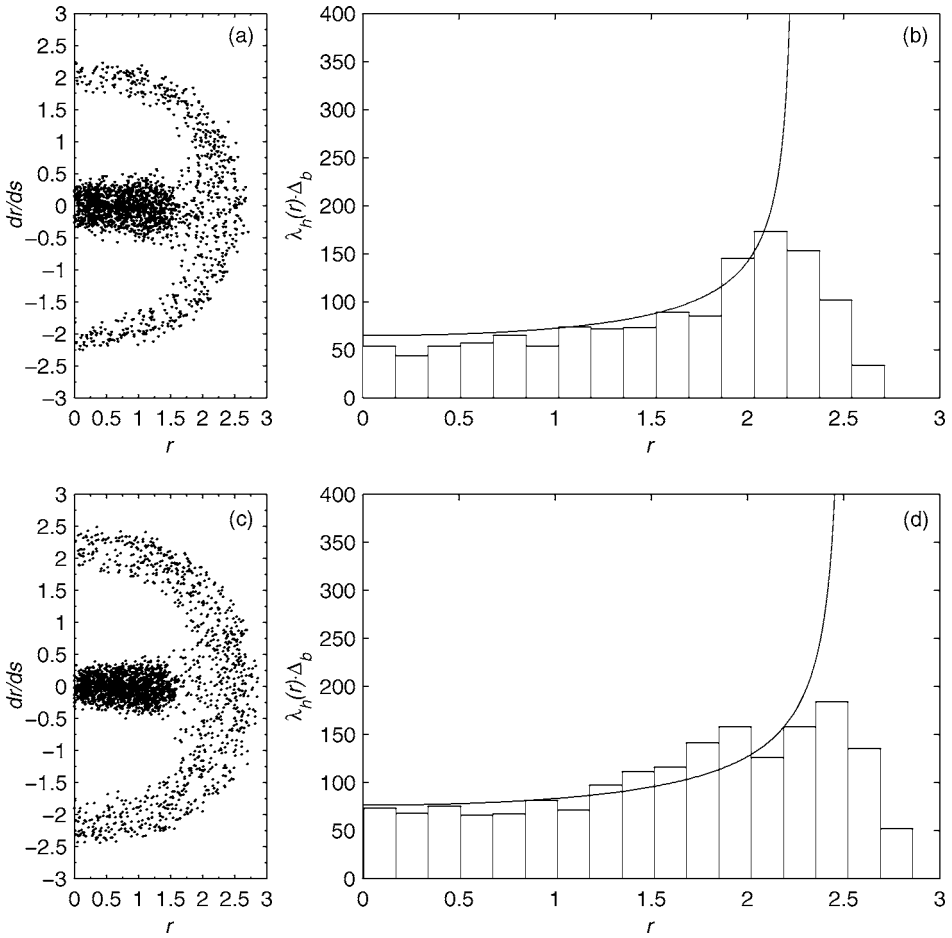

FIG. 5. phase-spaces corresponding to the full self-consistent N -particle simulations at $s\cong 800$ for (a) $r_0=1.8$ and (c) $r_0=2.0$. The histograms of beam halo particles for each one of these mismatches are, respectively, shown in panels (b) and (d), in which the analytical model is also plotted for comparison. $\Delta_b=0.1695$ is the size of the bins employed in the histograms.

These coefficients are shown in the next three rows of Table I. Considering the previous coefficients, it is possible thus to evaluate the fraction f of beam halo particles for each one of the initial beam mismatch values. The results for fraction f computed through the developed model are shown in the sixth row of this same table and can be compared with the results provided by the full simulations, shown in the row right below.

Being the obtainment of the fraction f the central point of the developed model, it is also convenient to plot its results together with the results provided by full simulations. From Fig. 3(a), it is possible to observe that as the initial beam mismatch r_0 decreases toward the equilibrium value $r_{eq}=1.0$, the difference between the results provided by the analytical model and the full simulations increases. This occurs because, in fact, as the initial mismatch r_0 assumes small values, the beam phase-space branch in which the halo particles lie changes its geometry, migrating from a semicircular to a semielliptical shape. This distortion in the semicircular branch of the beam phase-space can be observed in the snapshots of Figs. 3–5. For beams a little bit mismatched (including the case of mismatch values of $0<r_0<r_{eq}$), the difference between the model predictions and the simulations should increase considerably. Since all other beam quantities at equilibrium such as the beam envelope r_b and the beam emittance ε are just functions of the fraction f, it is expected that, also for these quantities, the large differences between the analytical model and the full simulations also occur for small values of r_0. The values for the beam envelope r_b and the emittance ε computed through the analytical model and the simulations are shown in remaining rows of Table I. As can be seen, the agreement shows to be nice.

Finally, for each one of the initial beam mismatches r_0, the halo particle density obtained from full simulations with that of the developed analytical model has also been compared. For this, histograms of the halo particle population from the full simulations have been calculated for each one of the initial beam mismatches r_0 considered in this work. These comparisons are presented in panel (b) of Fig. 3 and in panels (b) and (d) of Figs. 4 and 5. Again, it is possible to observe that a better agreement between the developed model and the full simulations is achieved for larger values of r_0, since just in these cases, actually, the beam phase-space region where the halo particles lie has a circular shape. Also, it can be noted that the developed model also reasonably describes the peak at $r=r_h$, which naturally appears in the full simulations. This is a consequence of the geometrical aspects of the resonances, in whose separatrix the beam halo particles predominantly are.

V. CONCLUSIONS

In this work, an analytical approach to obtain beam quantities such as the emittance, the envelope, and the fraction of particles that compose the halo at the beam's stationary state as a function of its initial mismatch has been pre-

sented. For simplification in the calculations, the present study has been restricted to the case of azimuthally symmetric and space-charge dominated beams with an initial step-function profile, evolving in an inner linear focusing channel permeated by a constant magnetic field. Nevertheless, the model can be directly employed to such other system parameters, as the type of magnetic focusing field, or system initial conditions, dictated by the initial beam distribution, without any consideration of symmetry. In general, the model helps to understand some basic physical aspects involved in the halo formation.

The key feature of the developed analytical model is the determination of the density of halo particles $n_h(r)$, mathematically expressed in Eq. (19), and which has been obtained through the assumption of phase-space invariance at the beam equilibrium. This assumption has been corroborated by the several full self-consistent N-particle simulations carried out, in which the splitting of the beam particles in at most two distinct populations of cold and hot particles naturally appears. It is convenient to remember that there is actually another kind of particle population, a warm one. Although this particle population has some importance in the understanding of the mechanisms behind the halo formation, to predict beam stationary quantities it can be neglected, since its energy contribution is small at the beam equilibrium. Also, the full simulations have demonstrated that the halo particle density $n_h(r)$ obtained in this work is also valid for many values of the initial beam mismatch r_0. The density of halo particles has in a compact manner all the information about the beam stationary state and thus, the connection with the nonstationary state can be readily performed with the aid of the equations for the beam conserved quantities. With this, the beam quantities of interest here at equilibrium could be obtained as function of just the initial beam mismatch and the fraction f of beam halo particles. This is an important conclusion since, to predict beam quantities at equilibrium, one does not need to understand the complete dynamics involved in the way particles are ejected from the initial cold beam, but just its amount f in the halo phase-space region. In fact, the fraction f is the weight factor of energy transfer from the macroscopic beam envelope oscillation to the microscopic chaotic movement of individual particles that composes the beam halo. Full simulations have assured this and also the model prediction that f is constant at the beam stationary state, which means, from energy conservation point of view, that no more energy exchange exists between the cold core and the hot halo at this time. In this sense, the fraction f also appears as a good indicator for the beam halo formation, being an alternative to the statistical quantity emittance. The physical meaning of f is directly related to the energy flux between the beam core and the beam halo.

The model results for the beam emittance, beam envelope, and the fraction of halo particles have presented nice agreement with the results originated from full simulations. The accordance has shown to be particularly better for higher beam mismatch values. In this case, the beam phase-space branch where the halo particles lie is really very close to a semicircular shape, matching the geometrical aspects considered in the construction of $n_h(r)$. However, as the mismatch decreases, the beam phase-space separatrix starts to deform toward a semielliptical shape, and thus the difference between the developed model and the full simulations grows. Yet, this seems not to be critical for $r_0 > 1.2$.

In this way, future works will contemplate the improvement of the expression for the density of halo particles $n_h(r)$ in the way of reducing the problem observed above. The assumption of an elliptical geometry for determining $n_h(r)$ will also expand its application to the case of mismatched beams without azimuthal symmetry, mathematically described by $\Delta_b \neq 0$. Also, another important result will be the obtainment of an analytical expression for coefficients of the polynomial of Eq. (28). This one will eliminate the only intermediate step in the model that has to be solved numerically, allowing to establish a closed expression for the fraction f.

ACKNOWLEDGMENTS

This scientific research has been done with the aid of the National Centre of Supercomputation of the Brazil's South Region (CESUP), located at the Federal University of Rio Grande do Sul (UFRGS).

Also, Roger Pizzato Nunes would like to dedicate special thanks and to register in this work the help provided by Dr. Tsuyoshi Tajima, from the Los Alamos National Laboratory (LANL), Los Alamos, NM. His promptness into quickly send research works from LANL has improved the quality of the references here employed.

Finally, this work has received financial support from the National Council for Scientific and Technological Development (CNPq), from the Fundação de Amparo à Pesquisa do Estado do Rio Grande do Sul (FAPERGS), both from Brazil, and from the Air Force Office of Scientific Research (AFOSR), Arlington, VA, under Grant No. FA9550-06-1-0345.

[1] A. Cuchetti, M. Reiser, and T. Wangler, in *Proceedings of the Invited Papers, 14th Particle Accelerator Conference*, San Francisco, CA, 1991, edited by L. Lizama and J. Chew (IEEE, New York, 1991), Vol. 1, p. 251; M. Reiser, J. Appl. Phys. **70**, 1919 (1991).
[2] R. A. Jameson, *Proceedings of the Particle Accelerator Conference*, Washington, DC (IEEE, New York, 1993), p. 3926; Los Alamos Report No. LA-UR-93-1209, 1993.
[3] R. L. Gluckstern, Phys. Rev. Lett. **73**, 1247 (1994).
[4] A. J. Lichtenberg and M. A. Lieberman, *Regular and Stochastic Motion* (Springer-Verlag, New York, 1992), p. 115.
[5] T. P. Wangler, K. R. Crandall, R. Ryne, and T. S. Wang, Phys. Rev. ST Accel. Beams **1**, 084201 (1998); J. S. O'Connell, T. P. Wangler, R. S. Mills, and K. R. Crandall, *Proceedings of the Particle Accelerator Conference*, Washington, DC (IEEE, New York, 1993), p. 3657.
[6] K. Fiuza, F. B. Rizzato, and R. Pakter, Phys. Plasmas **13**, 023101 (2006).
[7] R. P. Nunes, R. Pakter, and F. B. Rizzato, Phys. Plasmas **14**, 023104 (2007).
[8] R. C. Davidson and H. Qin, *Physics of Intense Charged Particle Beams in High Energy Accelerators* (World Scientific, Singapore, 2001), Chap. 6.
[9] R. P. Nunes and F. B. Rizzato, Proceedings of the 11th European Particle Accelerator Conference, Genoa, Italy, 2008, contribution ID 2322 (unpublished).
[10] R. P. Nunes and F. B. Rizzato, Proceedings of the 11th European Particle Accelerator Conference, Genoa, Italy, 2008, contribution ID 2322 (unpublished).